

## Prediction of foundations behavior by a stress level based hyperbolic soil model and the ZEL method

M. Veiskarami\*, M. Jahanandish, A. Ghahramani

Department of Civil and Environmental Engineering, Shiraz University, Shiraz, Iran

Received 2 October 2010, accepted in revised form 5 December 2010

---

### Abstract

In shallow foundations, the third bearing capacity factor,  $N_\gamma$ , has been found to show a decreasing tendency with increasing the foundation size. It is supported by experimental observations and related mainly to stress level dependent nature of the soil. On the other hand, the bearing capacity is often obtained theoretically without consideration of the foundation vertical displacements. In this study, a simple form of the stress level dependent hyperbolic soil model is presented and implemented in the Zero Extension Lines (ZEL) method to predict the bearing capacity and load-displacement behavior of shallow foundations. A computer code is developed for this study. A procedure to find the actual behavior of relatively large foundations based on laboratory and in situ small scale or plate load tests data is also presented. An existing experimental full scale load test is investigated and analyzed with the presented method to show the possibilities and advantages of the method in comparison with ordinary approaches. The results show that the presented method is applicable for practical problems to provide a more precise estimate of the bearing capacity of shallow foundations.

**Keywords:** Bearing capacity; Plasticity; Foundation; Load-displacement; Stress level; ZEL.

---

### 1. Introduction

Shallow foundations behavior is one of the major problems in geotechnical engineering. Several theoretical and experimental methods have been developed in the past decades to provide a good estimation of the bearing capacity of foundations. The well-known bearing capacity equation of Karl Terzaghi (1943) has been widely accepted for practical use, which is often presented in the following form [1]:

$$q_{ult} = cN_c + \bar{q}N_q + 0.5\gamma BN_\gamma \quad (1)$$

---

\* Corresponding author.

E-mail addresses: mveiskarami@shirazu.ac.ir (M. Veiskarami), mveiskarami@gmail.com (M. Veiskarami), jahanand@shirazu.ac.ir (M. Jahanandish), ghahrama@shirazu.ac.ir (A. Ghahramani)

In this equation,  $c$  is cohesion,  $\bar{q}$  is the surcharge pressure,  $B$  is the foundation width,  $\gamma$  is the soil density,  $q_{ult}$  is the ultimate bearing capacity and  $N_i$  coefficients are the bearing capacity factors as functions of soil friction angle. In shallow foundations, the third factor has the major contribution in the bearing capacity.

Many attempts have been made, based on limit theorems, in determination of the third factor,  $N_\gamma$ , by different assumptions resulting in a wide range for  $N_\gamma$  [1-9]. The third term suggests a linear increasing tendency in the bearing capacity of shallow foundations with increasing the foundation size. However, several researchers have observed and reported that the bearing capacity of shallow foundations does not increase with foundation size without bound and,  $N_\gamma$  decreases when the foundation size increases (De Beer, 1965; Ovesen, 1975; Kimura *et al.*, 1985; Bolton and Lau, 1989; Clark, 1998; Cerato, 2005; Cerato and Lutenegeger, 2007; Cerato and Lutenegeger, 2007; Kumar and Khatri, 2008; Yamamoto *et al.*, 2009) [10-19]. There are also other experimental methods based on small scale or in situ tests results, for prediction of shallow foundations behavior [20]. In practical cases, it is conventional to perform a small scale footing load test or a plate load test and extrapolate the results to larger foundations. Investigations of Fellenius and Altaee (1994) among other researchers showed that when such extrapolation is performed to predict the behavior of the prototype, based on small scale experiments, it requires a stress scale to be observed rather than a geometrical extrapolation alone [21]. The reason behind such observations can be related to the role of strains in soil mechanics and the concept of the stress level which affects the shear strength properties of soils, in particular, medium to dense sands and granular soils [22-25]. When soil behavior is very important for investigation of shallow foundations behavior, it was observed that the stress-strain behavior of sands can be approximated by a hyperbola (Kondor, 1963; Duncan and Chang, 1970) which is a basis for a hardening soil model arbitrarily used in many computer codes, e.g. PLAXIS [26-28]. Considering the role of strains in soil mechanics, many theoretical approaches without strain consideration, assuming a constant value of soil friction angle could provide over-conservative or unsafe bearing capacities; bearing capacity obtained from a load-displacement behavior seems to be more reliable and meaningful. Development of a proper approach to extrapolate the results of small scale footing load tests to larger foundations have been often a matter of concern and seems to be very useful in foundation engineering.

In this research, the Zero Extension Lines (ZEL) method has been employed in which, a relatively simple form of the hyperbolic soil model is implemented to predict shallow foundations behavior on granular soils. This method can be used for many plasticity problems in soil mechanics dealing with stresses, strains and displacement. The background and history of this method is well described by Anvar and Ghahramani (1997) and Jahanandish (2003) [29,30]. This study is expected to provide a methodology to enable extrapolation of small scale footings behavior to larger foundations considering the role of strains and the effect of stress level. A computed code has been developed for this research to predict foundations behavior by the presented approach.

## 2. Review on the ZEL method

Following Anvar and Ghahramani (1997) and Jahanandish (2003) there are two directions along which, increments of axial strains are zero which are defined as follow [29,30]:

Equations for the ZEL Directions:

$$\left\{ \begin{array}{l} \text{For +tive direction: } \frac{dz}{dr} = \tan(\psi + \xi) \\ \text{For -tive direction: } \frac{dz}{dr} = \tan(\psi - \xi) \end{array} \right. \quad \text{and} \quad \xi = \frac{\pi}{4} - \frac{\nu}{2} \quad (2)$$

In these equations,  $r$  and  $z$  are measures of horizontal and vertical directions (for both axis-symmetric and plane strain problems),  $\psi$  is the direction of principal normal strain (or stress, when coaxiality is assumed) with respect to the horizontal direction and  $\nu$  is soil angle of dilation.

Therefore, the plasticity equations can be derived along the two ZEL directions, namely plus ( $\varepsilon^+$ ) and minus ( $\varepsilon^-$ ) directions as one of the following forms which are equivalent [29,30]:

Anvar and Ghahramani (1997) Equations along the ZEL Directions:

$$\left\{ \begin{array}{l} \text{Along the minus (-) ZEL:} \\ dS - 2(S \tan \phi + c) \left( \bar{\alpha} d\theta + \bar{\zeta} \frac{\partial \psi}{\partial \varepsilon^+} d\varepsilon^- \right) = X \bar{\beta} (\tan \phi dz + \bar{\alpha} dx) - Z \bar{\beta} (\tan \phi dx - \bar{\alpha} dz) \\ + (S - c \tan \phi) \left( \tan \phi d\phi - \frac{1}{\cos \phi} \frac{\partial \phi}{\partial \varepsilon^+} d\varepsilon^- \right) + \left( \tan \phi dc - \frac{1}{\cos \phi} \frac{\partial c}{\partial \varepsilon^+} d\varepsilon^- \right) \\ \text{Along the plus (+) ZEL:} \\ dS + 2(S \tan \phi + c) \left( \bar{\alpha} d\theta + \bar{\zeta} \frac{\partial \psi}{\partial \varepsilon^-} d\varepsilon^+ \right) = -X \bar{\beta} (\tan \phi dz - \bar{\alpha} dx) + Z \bar{\beta} (\tan \phi dx + \bar{\alpha} dz) \\ + (S - c \tan \phi) \left( \tan \phi d\phi - \frac{1}{\cos \phi} \frac{\partial \phi}{\partial \varepsilon^-} d\varepsilon^+ \right) + \left( \tan \phi dc - \frac{1}{\cos \phi} \frac{\partial c}{\partial \varepsilon^-} d\varepsilon^+ \right) \end{array} \right. \quad (3)$$

Jahanandish (2003) Equations along the ZEL Directions:

$$\left\{ \begin{array}{l} \text{Along the minus (-) ZEL:} \\ dS + \frac{\partial T}{\partial \varepsilon^+} d\varepsilon^- - \frac{2T}{\cos \nu} (d\psi - \sin \nu \frac{\partial \psi}{\partial \varepsilon^+} d\varepsilon^-) = [f_r \cos(\psi - \xi) + f_z \sin(\psi - \xi)] d\varepsilon^- \\ \text{Along the plus (+) ZEL:} \\ dS + \frac{\partial T}{\partial \varepsilon^-} d\varepsilon^+ + \frac{2T}{\cos \nu} (d\psi - \sin \nu \frac{\partial \psi}{\partial \varepsilon^-} d\varepsilon^+) = [f_r \cos(\psi + \xi) + f_z \sin(\psi + \xi)] d\varepsilon^+ \end{array} \right. \quad (4)$$

In these equations,  $S$  is the mean stress,  $c$  and  $\phi$  are the soil shear strength parameters,  $\varepsilon^+$  and  $\varepsilon^-$  are measures of distance along positive and negative ZEL directions,  $X$  and  $Z$  are body and/or inertial forces in horizontal and vertical directions, and other parameters are defined as follow [29,30]:

$$T = (S \sin \phi + c \cos \phi), \quad \bar{\alpha} = \frac{1 - \sin \phi \sin \nu}{\cos \phi \cos \nu}, \quad \bar{\beta} = \frac{\cos \nu}{\cos \phi}, \quad \bar{\zeta} = \frac{\sin \phi - \sin \nu}{\cos \phi \cos \nu} \quad (5a)$$

$$\left\{ \begin{array}{l} f_r = X - \frac{n}{r} (\sigma_r - \sigma_\theta) \\ f_z = Z - \frac{n}{r} \tau_{rz} \end{array} \right. \quad \sigma_\theta = \sigma_3 \Rightarrow \left\{ \begin{array}{l} f_r = X - \frac{nT}{r} (1 + \cos 2\psi) \\ f_z = Z - \frac{nT}{r} \sin 2\psi \end{array} \right. \quad (5b)$$

Variations of soil shear strength parameters are included in the ZEL equations. These variations can be a result of soil non-homogeneity or variations in stress level at different points. Therefore, the effect of stress level on soil shear strength parameters can be considered in the ZEL method and hence, it can be utilized for the purpose of this research.

Directions of soil minor and major principal stresses are shown in Figure 1a. Zero Extension Lines directions are also shown in Figure 1b. Figure 1c, shows an element  $AB$  of the ZEL along which, axial strain is zero in conjunction with principal strains (and stresses) directions.

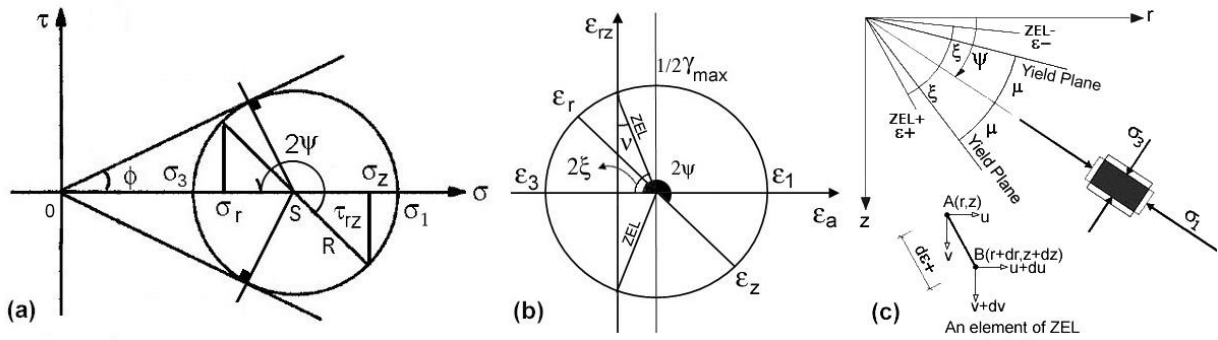


Figure 1. Mohr circles of stress and strain: a) Minor and major principal stresses and b) Minor and major principal strains with ZEL directions.

Since the Zero Extension Lines can work as rigid links between their start and end points, the horizontal displacement,  $u$  and vertical displacement,  $v$ , of any segment, like  $AB$ , should be normal to  $AB$  and therefore, the following expression is resulted [29,30]:

$$\frac{du}{dv} = -\frac{dz}{dr} \tag{6}$$

This equation can be written in a finite difference form and if a displacement boundary is known, the strain and displacement fields will be found. Relationship between soil maximum shear strain and  $\sin\phi_{mob}$  can then be used to find a complete load-displacement behavior for foundations or retaining walls as indicated in the literature [29,30]. Numerical solution technique is also well described by Anvar and Ghahramani (1997) or Jahanandish (2003) [29,30].

### 3. Deformation computation

The main property of the ZEL net can be employed to find the velocity field. Since the Zero Extension Lines are lines of zero axial strains, the ZEL would be used as rigid links that can move or rotate without axial deformation. As a consequence, for a given deformation boundary condition, the generated displacements in the ZEL net can be computed using the finite difference form of equation 7 for any two successive points. For example a rotating boundary is shown in Figure 2. The left boundary is held to be fixed against translation. To find the final position of point, say,  $B_2$  after deformation it is sufficient to rewrite equation 7 in a finite difference form. Knowing the displacements of points  $A_2$  and  $A_3$ , the displacements of point  $B_2$ , i.e.,  $u_{B2}$  and  $v_{B2}$  will be obtained [29,30]. A summary of finite difference forms of the equations are presented in Appendix A.

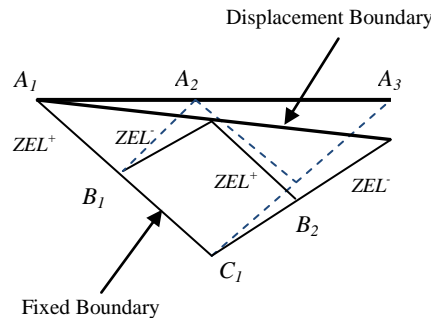


Figure 2. A schematic deformed ZEL net.

### 3.1. Developed computer code

To solve the ZEL equations by taking the effect of stress level into account, a computer code in MATLAB has been developed for this research. The developed code consists of several subroutines in which, input data are inserted and the equations are solved. First, the ZEL net is constructed by assuming an initial value for soil friction angle ( $\phi$ ) and soil dilation angle. Since soil angle of dilation remains constant during a major part of shearing [31], the ZEL net can be assumed also to remain unchanged for the entire load-displacement analysis. Initial value of soil friction angle is assumed to be equal to critical state soil friction angle,  $\phi_{c.s.}$ , regarding the fact that the ZEL net should predict the ultimate load in which, mobilized soil shear strains have been reached to the corresponding value for mobilization of a critical state soil friction angle.

Then, a  $k_0$  procedure is then performed to initialize the stress field, since the soil mobilized friction angles at the first step of loading are stress level dependent. In the next step, an incremental vertical displacement is applied on the foundation and the velocity (displacement) field is computed. Based on the velocity field, strain field can be computed remembering that the ZEL properties stated earlier. Having known the initial stresses and developed strains at the first step of loading, the corresponding soil mobilized friction angle,  $\phi_{mob}$ , which is a function of stress level and soil maximum shear strain is computed at every point within the ZEL field. The dependency of soil friction angle to both stress level and maximum shear strain can be considered either by curve fitting to the laboratory shear test results or by implementing a soil model which will be discussed later. The stress field (which can be calculated from the ZEL equations) and corresponding foundation pressure are then computed and the current obtained stress field is used for further steps of loadings and displacements. In each part, an iterative procedure is carried out for convergence. Finally, the entire load-displacement curve will be obtained. The procedure is outlined in the presented flowchart of Appendix A.

## 4. Application of the hyperbolic soil model

As stated before, original hyperbolic soil model is common in most of geotechnical analyses, particularly, in case of stress-controlled loading. Here it can be used as a basis for modeling soil behavior in laboratory shear tests. For the purpose of this work and considering the hyperbolic form of the stress-strain curve in most of laboratory shear tests, based on formulation presented for this model, the stress-strain curve can be approximated by a hyperbola with the following general form for a triaxial shear test [26-28]:

$$\varepsilon_1 = \frac{1}{2E_{50}} \frac{q}{1 - q/q_a} \quad (7)$$

In this equation,  $\varepsilon_1$  is axial strain,  $q$  is deviatoric stress ( $\sigma_1 - \sigma_3$ ),  $q_a$  is the asymptote of the hyperbola obtained from test results (which can be equal or more than ultimate value of  $q$ ) and  $E_{50}$  is the confining stress dependent stiffness modulus for primary loading and is given by the following equation for a general condition [26-28]:

$$E_{50} = E_{50}^{ref} \left( \frac{c \cos \phi + \sigma'_3 \sin \phi}{c \cos \phi + p^{ref} \sin \phi} \right)^m \quad (8a)$$

This equation can be reduced to the following form for cohesionless soils:

$$E_{50} = E_{50}^{ref} \left( \frac{\sigma'_3}{p^{ref}} \right)^m \quad (8b)$$

In this equation,  $E_{50}^{ref}$  is the reference stiffness modulus at reference confining pressure defined by  $p^{ref}$  and  $m$  as an exponent [26-28]. Reference confining pressure is 100kPa for example in SI units. The value of  $m$  ranges between 0.5 and 1.0; for example, Janbu (1963) for Norwegian sands and silt found the value of  $m$  to be equal to 0.5 [26-28,32]. The hyperbolic stress-strain relationship is shown in Figure 3.

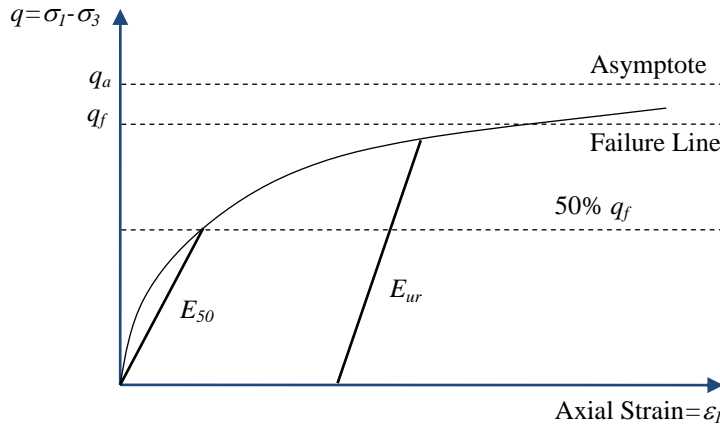


Figure 3. Representation of a hyperbolic soil model.

In this study, to simulate shear stress-shear strain relationship, first, the following general form of the hyperbolic equation is rewritten:

$$\epsilon_1 = A_1 \frac{q}{1 - q/q_a} \tag{9}$$

In this equation, parameter  $A_1$  is equal to  $1/2E_{50}$ , and can also be determined by plotting the initial slope of the stress-strain curves obtained in laboratory shear tests versus confining pressure. The  $q-\epsilon_1$  relationship can also be rearranged in the following form:

$$q = \frac{\epsilon_1}{A_1 + \frac{\epsilon_1}{q_a}} \tag{10}$$

Since in the ZEL method the relationship between  $\gamma_{max}$  and mobilized soil friction angle,  $\phi_{mob}$ , is required. These terms can be derived from the hyperbolic soil model as follow:

$$\gamma_{max} = \frac{2\epsilon_1}{(1 + \sin \nu)} \tag{11a}$$

And

$$\sigma_1 = \sigma_3 \tan^2 \left( \frac{\pi}{4} + \frac{\phi_{mob.}}{2} \right) \tag{11b}$$

$$\Rightarrow \phi_{mob.} = 2 \arctan \left( \sqrt{\frac{\sigma_1}{\sigma_3}} \right) - \frac{\pi}{2} \tag{11c}$$

In these equations  $\nu$  is soil angle of dilation. Regarding that  $\sigma_3$  is constant during a triaxial test, it is possible to define a stress ratio,  $f$ , as  $f=q/\sigma_3$  and substitute this definition in the hyperbolic soil model to develop a relatively simple equation for application in the ZEL method:

$$f = \frac{\gamma_{max}}{A_2 + \frac{\gamma_{max}}{f_a}} \quad \text{or} \quad \gamma_{max} = A_2 \frac{f}{1 - \frac{f}{f_a}} \quad (12)$$

In which  $A_2$  is a parameter defining the hyperbola and  $f_a$  is the asymptote of the hyperbola. The relationships between stresses and strains are shown in Mohr's circles of stresses and strains in Figure 4.

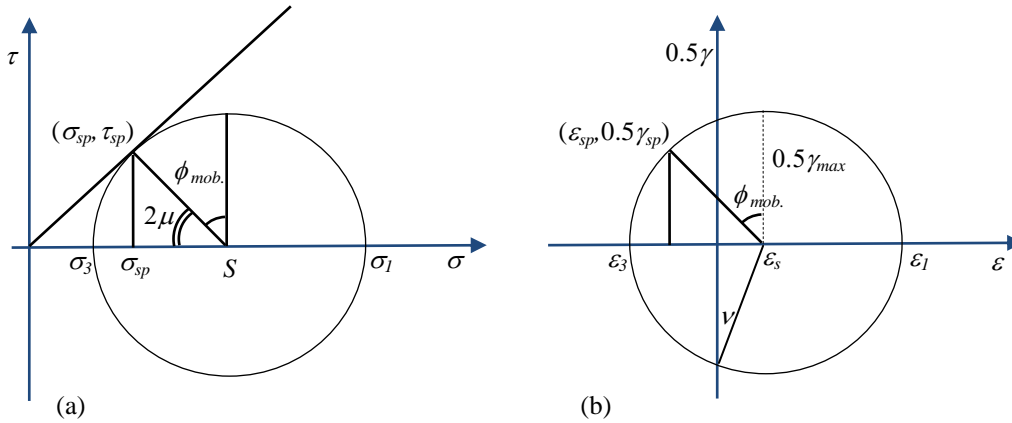


Figure 4. Mohr's circle of stresses and strains for a general stress and strain configuration.

Considering stress level dependency of parameters  $A_1$  (and  $A_2$ ) for cohesionless soils:

$$A_1 = \frac{1}{2E_{50}} = \frac{1}{2E_{50}^{ref} \left(\frac{\sigma_3}{P_a}\right)^m} \quad (13)$$

Therefore, it is possible to define the following values for the new form of the hyperbolic model:

$$A_2 = A_2^{ref} \left(\frac{\sigma_3}{P_a}\right)^m \quad (14)$$

According to stress level dependency of soil friction angle [22-24], this dependency can be defined as follow:

$$\phi_{max} = B_1 - B_2 \ln\left(\frac{\sigma_3}{P_a}\right) \quad (15)$$

In this equation,  $\phi_{max}$  is maximum mobilized soil friction angle which determines the asymptote of the hyperbolic function,  $B_1$  and  $B_2$  are model parameters and  $P_a$  is reference (often atmosphere) pressure. Therefore, stress level dependent asymptote parameter,  $f_a$ , can be easily determined at each level of confining pressure,  $\sigma_3$ .

Now, a stress level dependent hyperbolic soil model is ready to be implemented in the ZEL method to predict foundations behavior. In order to provide an actual load-displacement curve of shallow foundations, it is possible to find the corresponding appropriate soil stress-strain relationship. It can be done by back calculation of the results for one or two small scale load tests. It will be discussed further through a comprehensive example to show the procedure.

### 5. Geometry of the problem and boundary conditions

Prediction of foundations behavior by the ZEL method is a boundary value problem in soil mechanics in which, the bearing pressure beneath a foundation is determined at each

incremental vertical displacement. There are several assumptions by the researchers to deal with the boundary conditions assumed for different types of foundations. Developed computer code for this research, is capable of solving both plane strain and axi-symmetric problems with smooth and rough bases. For rough base foundations, standard boundary condition of Bolton and Lau (1993) has been accepted and used. It is remarkable that when the third bearing capacity factor,  $N_\gamma$ , is aimed to be found, it is necessary to perform further assumption to deal with the surcharge pressure over the ground surface. Presence of such surcharge pressure is necessary to prevent trivial solution of the partial differential equation set of the ZEL method.

Bolton and Lau (1993) carried out a study on the effect of the surcharge pressure on computed  $N_\gamma$ , and presented a dimensionless factor,  $\Omega$ , defined as the ratio of the surcharge pressure,  $q$ , to  $\gamma B$ . They stated that if this factor is equal or less than 1.0, the effect of surcharge pressure leads to less than 20% error in calculation of the bearing capacity factor,  $N_\gamma$ , which seems to be acceptable for practical purposes [5]. They suggested using a rigid triangular wedge (or cone, in axi-symmetric problems) as shown in Figure 5 and following Meyerhof (1963) inclined at angle  $\alpha$  equal to  $\pi/4+\phi/2$  [2,5].

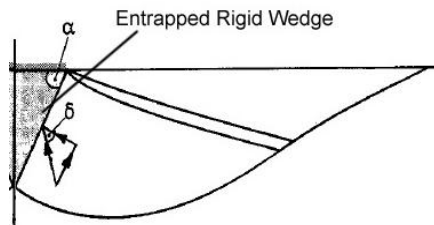


Figure 5. Failure mechanisms for a rough base foundations assumed by Bolton and Lau (1993) [5].

## 6. Prediction of foundations behavior

At this point, the behavior of shallow foundations is investigated, first by using the conventional method and then by suggested procedure based on the stress level dependent hyperbolic soil model. To do this, an existing foundation load test data is represented. There are many difficulties in carrying full scale load tests on relatively large foundations and there are very few large scale foundation load tests in the literature known to the authors. An exception is the large scale footing load test in Texas A&M University, Texas, U.S.A., in 1994, which has been represented for this study.

An experimental program was performed in Texas A&M University, in 1994, to investigate the load-displacement behavior of shallow foundations and compare different methods in finding the actual ultimate load of the foundations as a competition. Large spread square foundations 1.0m, 1.5m, 2.5m and 3.0m wide were tested. The footing thicknesses were 1.2m to provide relatively rigid foundations. Details of this program were presented by FHWA (1997), Briaud and Gibbens (1999) and Briaud (2007) [33-35]. Subsoil condition was mainly consisted of sand with properties summarized in Table 1 [33].

Table 1. Summary of soil properties for foundation load tests at Texas A&M University [33].

Depth	$G_s$	$\gamma_{d-min}$ ( $kN/m^3$ )	$\gamma_{d-max}$ ( $kN/m^3$ )	$e_{min}$	$e_{max}$	$D_{10}$ (mm)	$D_{30}$ (mm)	$D_{50}$ (mm)	$D_{60}$ (mm)
0.6m	2.64	13.35	13.66	0.65	0.94	0.1*	0.15*	0.2*	0.3*
3.0m	2.66	15.70	16.10	0.62	0.91				

\* Approximate value



The laboratory shear tests were performed at confining pressures of 34kPa, 138kPa and 345kPa. Critical state soil friction angle was estimated between  $34.2^\circ$  to  $36.4^\circ$  degrees. Regarding the results of triaxial tests, soil angle of dilation was approximately obtained to be  $10^\circ$  to  $15^\circ$  and the value of  $12^\circ$  has been assumed for this study.

## 7. Analysis without stress level dependency consideration

First, the foundations behaviors were modeled with a unique soil stress-strain curve regardless of stress level or foundation size. To do this, the results of the triaxial shear tests were recompiled for using in the ZEL method. The detail has been presented by Veiskarami (2010) [36]. The results have been represented in terms of  $\sin \phi_{mob} - \gamma$  relationship which is required for the ZEL method as shown in Figure 6. In this way, stress level dependency is not considered and variation of soil mobilized friction angle at each point was considered to be only a function of soil maximum shear strain during the load-displacement analyses. The analyses have been performed for different size foundations described earlier. The results of the analyzed cases for 1.0m wide and 3.0m wide foundations are shown in Figure 7 and Figure 8. In these figures, the ZEL net and the deformed mesh at the final stage of the loading has been shown. It is remarkable that the tested square foundations were analyzed with equivalent circular foundations in an axy-symmetric model.

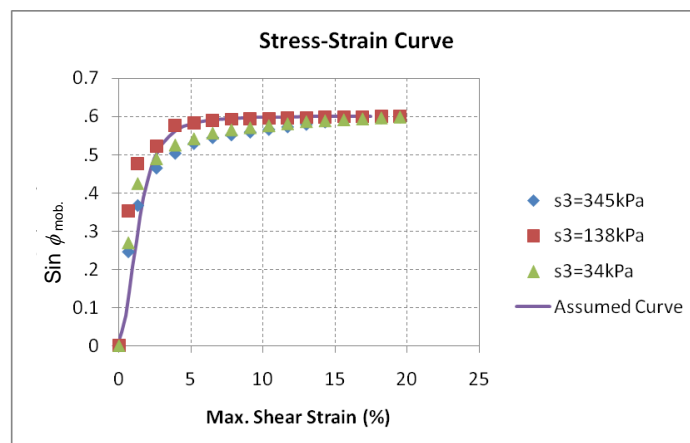


Figure 6. Stress-strain curve developed for the purpose of this study.

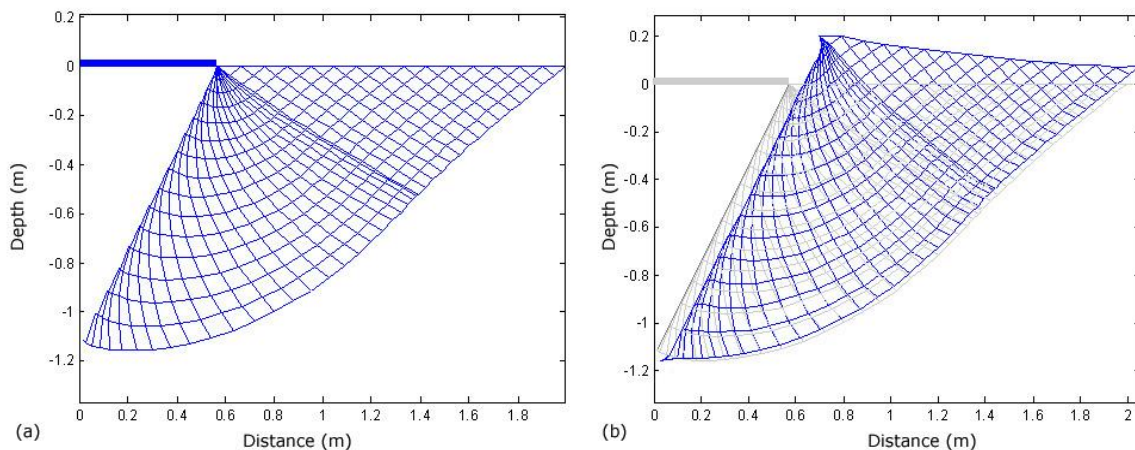


Figure 7. a) ZEL net for foundation of 1.0m width and b) deformed net.

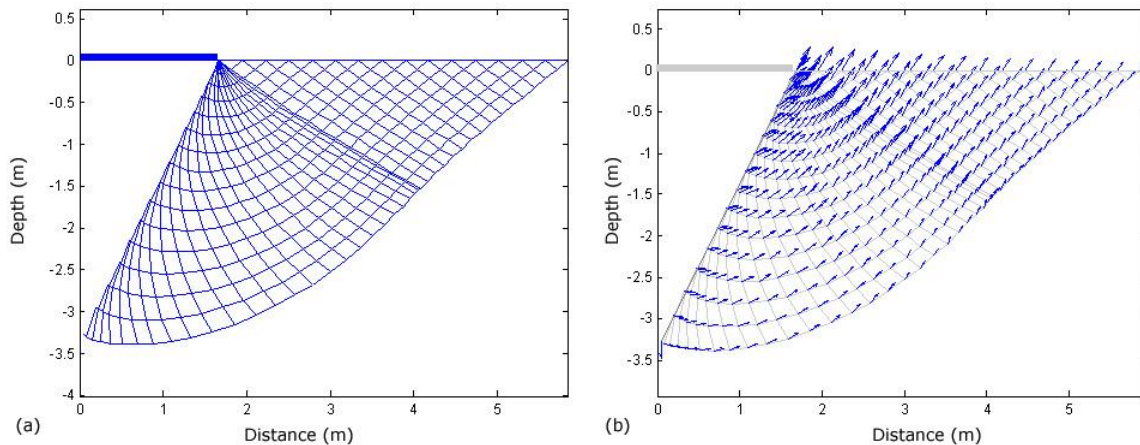


Figure 8. a) ZEL net for foundation of 3.0m width and b) velocity field.

Figure 9 shows the load-displacement curves obtained from the analyses in comparison with experimental data. It is clear that the predicted loads for relatively small foundations are proper, however, when the size increases, the predicted values located well above the experimental data. One of the important reasons behind this observation, among other possible reasons, can be related to the triaxial tests. In laboratory triaxial tests, the samples had not been tested at sufficiently high confining pressures to be representative of the entire stress levels in soil under different size foundations and at a wide range of applied stresses (as high as, say, 1000kPa). Thus, the tested confining pressures do not cover the entire confining pressures developed in the soil for foundations of different sizes and as a consequence, the predictions are not precise enough.

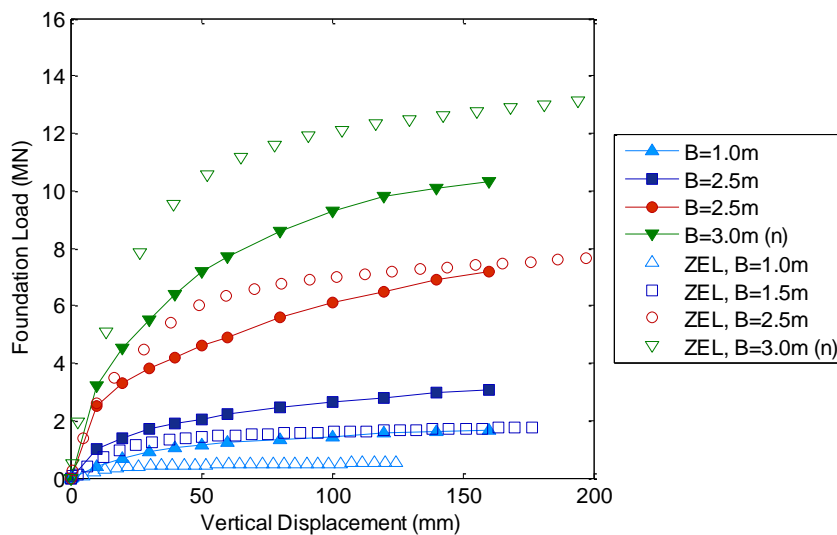


Figure 9. Load-displacement curves for Texas A&M (1994) footing load tests (prediction and experiments).

### 8. Analysis with stress level dependency consideration

To obtain better results, the previously described hyperbolic soil model was employed. As it was stated before and in order to find an appropriate load-displacement curve of shallow foundations, it is possible to find the corresponding appropriate soil stress-strain relationship. It can be done by back calculation of the results for one or two small foundation load tests.

Such procedure can be performed for series of small scale footing or plate load tests in practice and calibrating the model to take the effect of stress level into account.

To show the procedure, the results of the foundation load tests at Texas A&M University (1994) have been reutilized and the computations have been performed for these tests results:

- First, an initial soil stress-strain hyperbolic curve is constructed; it can be obtained from standard shear test results for the average applied stress in the laboratory. For instance, the stress-strain curve obtained from laboratory shear test data can be used. Triaxial tests have been performed at confining stresses of 34kPa, 138kPa and 345kPa with average confining stress value of 190kPa. Therefore, this curve and the coefficients can be considered to be corresponding to 190kPa mean confining pressure. The coefficients have been obtained by curve-fitting procedure. It is shown in Figure 10 in comparison with experimental data. The initial parameters are as follow for the primary hyperbolic curve:

$$f_a=3.5 \text{ and } A_2=0.5$$

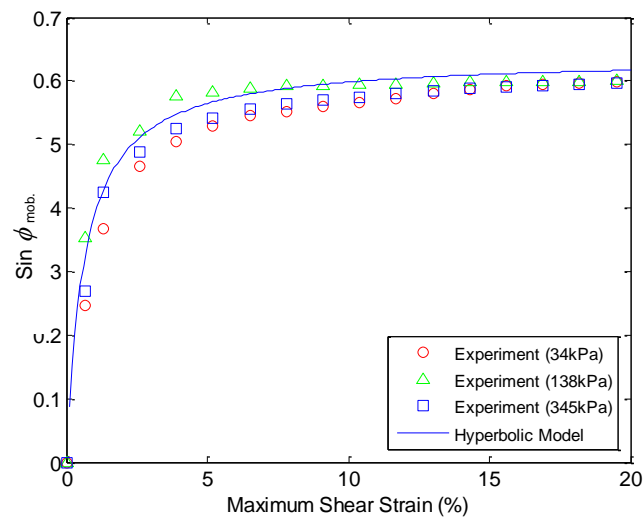


Figure 10. Stress-strain curve for the primary hyperbolic curve.

- Now, having known the results of some foundation load tests (at least two), the family of hyperbolic curves for different stress levels can be obtained. It is sufficient to find the values of  $B_1$  and  $B_2$  by a model calibration scheme. To do this, by a trial and error procedure, the foundation load-displacement curves are computed and compared with experimental results in such a way that computed and experimental results coincide as far as possible. Figure 11 shows the predicted and experimental results for 1.0m wide and 1.5m wide (with equivalent diameters of 1.13m and 1.84m consequently) foundations tested in Texas A&M University (1994). The analyses suggested taking the approximate values of  $B_1=68$  and  $B_2=5.8$ .

Family of hyperbolic curves at different confining pressures is also shown in Figure 12.

- Now, the model is calibrated and it can be used for further predictions. Figure 13 shows the load-displacement curves obtained for foundations of larger sizes by the presented procedure in comparison with existing experimental data. It is obvious that the results are in good agreement with experimental observations and hence, the obtained hyperbolic soil model and its associated parameters can be considered as a suitable model to describe and predict load-displacement behaviors of these foundations.

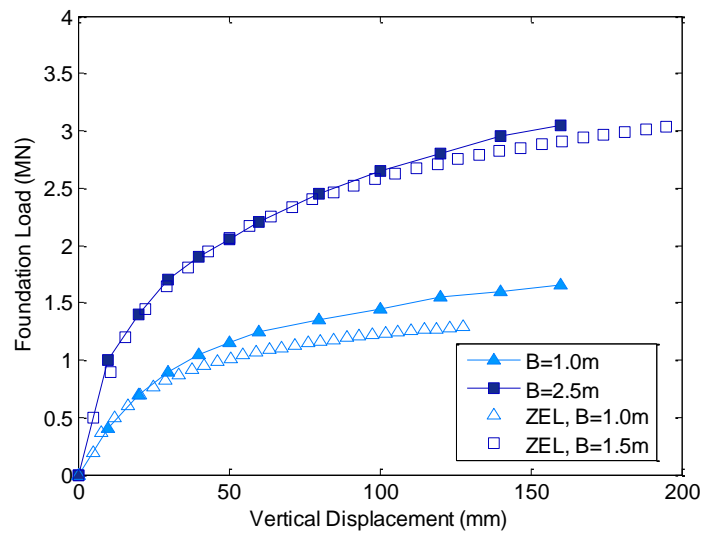


Figure 11. Model calibration with the two smallest foundations.

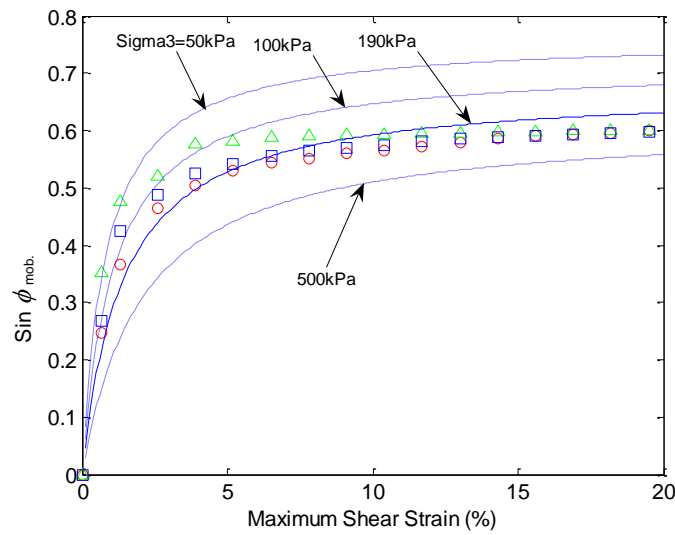


Figure 12. Family of hyperbolas.

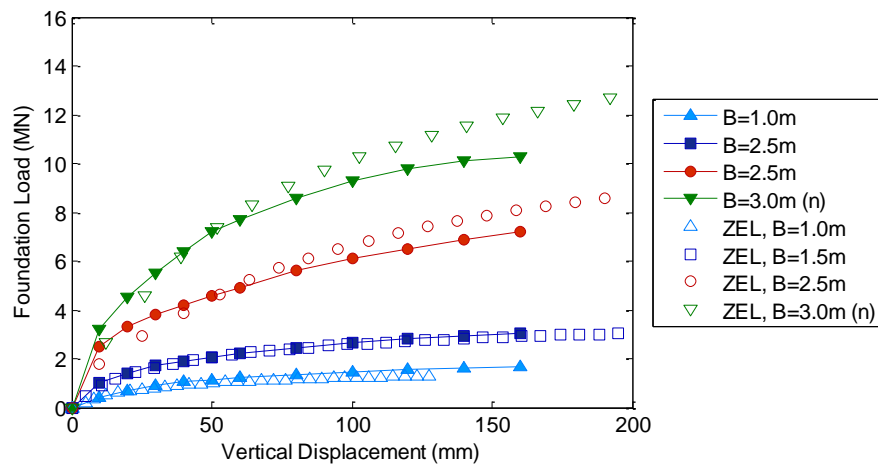


Figure 13. Results of the load-displacement predictions for the large size foundations.

In smaller foundations, computed bearing pressures based solely on the laboratory shear tests data, showed lower values in comparison with experimental data. In contrast for larger foundations, the computed values are relatively high when they are obtained only from laboratory shear tests results. It reveals the inadequacy of laboratory shear tests results for prediction of foundations behavior when they do not cover the entire range of experienced stresses and effect of stress level is not properly included. As a result, the stress level dependency of soil shear strength should be taken into account to obtain better and more realistic predictions. Another important conclusion is that the foundation pressure ratios (ultimate bearing pressure of these foundations normalized to  $\gamma B$ ), has a linear relationship with foundation size when plotted on a log-log scale graph. It is shown in Figure 14 in which, foundation pressure ratios for 10% of footing dimension (according to Briaud and Jeanjean, 1994), or ultimate values reported in the tests (if lower), have been computed [37]. Consistency of the results with previous observations indicates the important role of stress level in scaling the results of a small foundation to larger one.

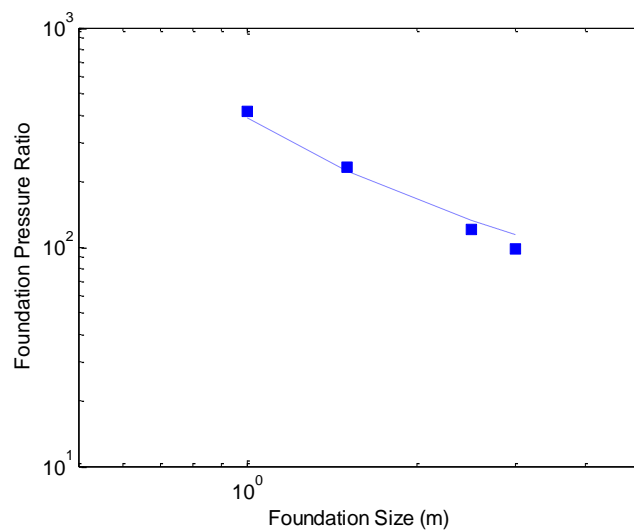


Figure 14. Decreasing tendency in foundations bearing capacity for Texas A&M University foundation load test program (1994).

At this point, an important conclusion can be made: while actual bearing capacity of foundations is required, estimations based on load-displacement behavior, i.e. with regard to the role of strains, provide better results rather than theoretical approaches through which, no consideration to the stress level dependency and influence of strains are considered. As a rough estimation, using the laboratory experimental data for the previous foundation load test program, the bearing capacity factor,  $N_\gamma$ , has been calculated based on Bolton and Lau (1993) suggested values for rough base circular foundations. Regarding the values of  $\phi$  ranging between  $34.2^\circ$  and  $36.4^\circ$ , with an average value of  $35.3^\circ$ , the average bearing capacity factor,  $N_\gamma$ , will be obtained to be equal to 85. Table 2, shows the corresponding ultimate pressures based on these values for  $N_\gamma$  and values obtained from the ZEL method.

Table 2. Summary of soil properties for foundation load tests at Texas A&M University.

Foundation Width	Experiments	Ultimate Load ZEL	Bolton and Lau (1993)	Equivalent Friction Angle*	Soil
1.0m	1.6MN	1.5MN	0.65MN	$39.4^\circ$	
1.5m	3.0MN	2.9MN	2.2MN	$36.6^\circ$	
2.5m	7.3MN	7.9MN	10.2MN	$33.3^\circ$	
3.0m	10.2MN	12.3MN	17.7MN	$32.3^\circ$	

\* These values are obtained from Bolton and Lau (1993) suggested values by back analysis

Comparison of the results reveals that when using a constant value of soil friction angle based on the theoretical bearing capacity formula, the obtained values are conservative for small size foundations, whereas in larger foundations, the results may be unsafe. Even more difference is expected to be observed for foundations with considerable dimensions. For example, if the decrease in foundation pressure ratio is approximated by a linear function of foundation size on a log-log plot, for a very large foundation, namely 10m wide, the analysis show that the maximum ultimate load should be roughly around 230MN while it is obtained to be approximately around 650MN when the value of  $N_\gamma$  is assumed to be equal to 85 which is well above the possible ultimate load over such foundation. It is remarkable while using the minimum (or maximum) soil friction angle in determination of  $N_\gamma$  may improve the results for some cases, the differences will be more significant in other cases regarding the variations of equivalent soil friction angles computed in this table for all cases. As a result, it seems that there is no reliable tool for selecting the appropriate value of soil friction angle and as a consequence, load-displacement curve prediction through similar analyses may be one of the useful methods for better estimation of the ultimate bearing capacity.

Therefore, selection of an appropriate value for the bearing capacity of shallow foundations seems a rather more difficult task than it appears to be, when the effect of foundation size and stress level should be taken into account. As a matter of fact, the main idea behind using the stress level based ZEL method is to provide the possibility to predict the ultimate bearing pressure of foundations through the foundation behavior prediction rather than solving the equilibrium and yield equations regardless of strains and stress level. The results of this study show that the presented procedure can be used to predict the foundations behavior with adequate precision and estimate the ultimate load of shallow foundations with reasonable agreement with experimental observations.

## 9. Conclusions

In this study, the effect and importance of the stress level in foundations behavior has been studied by development of a stress level based hyperbolic soil model implemented in the ZEL method. Among a few number of large scale footing load tests found in the literature, the full scale load tests performed in Texas A&M University in 1994 was recompiled and investigated. First, the laboratory shear tests data has been used to predict foundations behavior. The results showed that since the triaxial test data do not cover the entire range of experienced stresses in the soil, induced by different size foundations, predictions are relatively poor. The reason was found to be the inadequacy of laboratory shear test data; they were not a representative of the entire soil body experiencing higher levels of stress under different size foundations. In order to obtain a better prediction of foundations behavior, the procedure of using a stress level dependent hyperbolic soil model was described and the procedure was employed in the ZEL method.

Model calibration (computation of the model parameters) has been performed by a back calculation procedure for two foundations of different sizes. The calibrated model was then utilized to predict the behavior of other foundations in that group, larger in size. The obtained results showed reasonably good agreement with the experimental data. Further study revealed that the ultimate pressure obtained from the load-displacement behavior prediction, considering the effect of the stress level and foundation load-displacement behavior is more accurate and meaningful. In contrast, estimation of the ultimate load based solely on the solution of the stress field alone, without further consideration of the strain and stress level effects failed to estimate the true ultimate load. Such results when a constant value of  $N_\gamma$  is used for foundations of different sizes can be either over-conservative or unsafe, depending on many factors as well as the selected values of the soil friction angle, and, in particular, the

foundation size. However, the presented methodology is expected to overcome these shortcomings. Moreover, the presented approach is rather simple and applicable in many cases by taking both geometric and stress scales into account in extrapolation of the small scale footing load test results to large scale foundations. As a conclusion, the bearing capacity determined from a load-displacement curve and stress level consideration, has better agreement with experimental observations. On the other hand, the presented procedure works well in presence of at least two small scale footing (or plate) load test results to predict the behavior of larger foundations.

## References

- [1] K. Terzaghi, *Theoretical Soil Mechanics*, John-Wiley and Sons Inc., NY, 1943.
- [2] G.G. Meyerhof, Some recent research on the bearing capacity of foundations, *Can. Geotech. J.* 1 (1963) 16-26.
- [3] J.B. Hansen, A revised and extended formula for bearing capacity, *Danish Geotechnical Institute, Copenhagen, Bulletin* 28 (1970) 5-11.
- [4] A.S. Vesić, Analysis of ultimate loads of shallow foundations, *Journal of the Soil Mechanics and Foundations Division*, ASCE, 99 (1973) 45-73.
- [5] M.D. Bolton and C.K. Lau, Vertical bearing capacity factors for circular and strip footings on Mohr-Coulomb soil, *Can. Geotech. J.* 30 (1993) 1024-1033.
- [6] R.L. Michalowski, An estimate of the influence of soil weight on bearing capacity using limit analysis soils and foundations, *Japanese Geotechnical Society*, Vol. 37, No. 4, Dec. (1997) 57-64.
- [7] J. Kumar,  $N_\gamma$  for rough strip footing using the method of characteristics, *Can. Geotech. J.* 40 (3) (2003) 669–674.
- [8] J. Kumar and P. Ghosh, Bearing Capacity Factor  $N_\gamma$  for ring footings using the method of characteristics, *Can. Geotech. J.* 42 (2005) 1474-1484.
- [9] M. Hjiiaj, A.V. Lyamin and S.W. Sloan, Numerical limit analysis solutions for the bearing capacity factor  $N_\gamma$ , *Int'l Journal of Solids and Structures*, Elsevier, 42 (2005) 1681-1704.
- [10] E.E. De Beer, Bearing capacity and settlement of shallow foundations on sand, *In Proc. of the Bearing Capacity and Settlement of Foundations Symposium*, Duke University, Durham, N.C. (1965) 15-34.
- [11] N.K. Ovesen, Centrifugal testing applied to bearing capacity problems of footings on sand, *Géotechnique* 25 (2) (1975) 394-401.
- [12] T. Kimura, O. Kusakabe and K. Saitoh, Geotechnical model tests of bearing capacity problems in a centrifuge, *Géotechnique* 35 (1) (1985) 33-45.
- [13] M.D. Bolton and C.K. Lau, Scale effect in the bearing capacity of granular soils, *Proc. the 12<sup>th</sup> Int'l Conf. Soil Mech. Found. Eng.*, Rio De Janeiro, Brazil (1989) Vol. 2 895-898.
- [14] J.I. Clark, The settlement and bearing capacity of very large foundations on strong soils: 1996 R.M. Hardy keynote address, *Can. Geotech. J.* 35 (1998) 131-145.
- [15] A.B. Cerato, Scale effect of shallow foundation bearing capacity on granular material, *Ph.D. Dissertation*, University of Massachusetts Amherst (2005).
- [16] A.B. Cerato, and A.J. Lutenecker, Bearing capacity of square and circular footings on a finite layer of granular soil underlain by a rigid base, *Journal of Geotechnical and Geoenvironmental Engineering*, ASCE, Vol. 132, No. 11, Nov. (2006) 1496-1501.
- [17] A.B. Cerato, and A.J. Lutenecker, Scale effects of shallow foundation bearing capacity on granular material, *Journal of Geotechnical and Geoenvironmental Engineering*, ASCE, Vol. 133, No. 10, Oct. (2007) 1192-1202.

- [18] J. Kumar and V.N. Khatri, Effect of footing width on bearing capacity factor  $N_\gamma$ , *Journal of Geotechnical and Geoenvironmental Engineering*, ASCE, Vol. 134, No. 9., Sep. (2008) 1299-1310.
- [19] N. Yamamoto, M.F. Randolph and I. Einav, Numerical study of the effect of foundation size for a wide range of sands, *Journal of Geotechnical and Geoenvironmental Engineering*, ASCE, Vol. 135, No. 1, Jan. (2009) 37-45.
- [20] A. Eslami, and M. Gholami, Analytical model for the ultimate bearing capacity of foundations from cone resistance, *Scientia Iranica Journal*, Sharif University of Technology Press., Vol. 13, 3 (2006) 223-233.
- [21] B.H. Fellenius and A. Altaee, Stress and settlement of footings in sand, *In Proc. of the American Society of Civil Engineering, ASCE, Conference on Vertical and Horizontal Deformations for Foundations and Embankments, Geotechnical Special Publication, GSP, No. 40, College Station, TX, (June 16-18, 1994) Vol. 2 1760-1773.*
- [22] R.D. Holtz and W.D. Kovacs, *An Introduction to Geotechnical Engineering*, Prentice-Hall Press, 1981.
- [23] M.D. Bolton, The strength and dilatancy of sands, *Géotechnique* 36 (1986) 65-78.
- [24] J. Kumar, K.V.B.S. Raju, and A. Kumar, Relationships between rate of dilation, peak and critical state friction angles, *Indian Geotechnical Journal* 37 (1) (2007) 53-63.
- [25] K.H. Roscoe, The influence of strains in soil mechanics, Tenth Rankine Lecture, *Géotechnique* 20 (2) (1970) 129-170.
- [26] R.L. Kondor, A hyperbolic stress strain formulation for sands, *2<sup>nd</sup> Pan. Amer. ICOSFE, Brazil, Vol. 1, (1963) 289-324.*
- [27] J.M. Duncan and C.-Y. Chang, Nonlinear analysis of stress and strain in soil, *Journal of the Soil Mechanics and Foundation Engineering Div., ASCE, Vol. 96 (1970) 1629-1653.*
- [28] PLAXIS, *Materials Model Manual*, URL: <http://www.plaxis.nl/> (2005).
- [29] S.A. Anvar and A. Ghahramani, Equilibrium equations on zero extension lines and their application to soil engineering, *Iranian Journal of Science and Technology (IJST)*, Shiraz University Press., Transaction B Vol. 21, 1 (1997) 11-34.
- [30] M. Jahanandish, Development of a zero extension line method for axially symmetric problems in soil mechanics, *Scientia Iranica Journal*, Sharif University of Technology Press., Vol. 10, 2 (2003) 1-8.
- [31] R.G. James and P.L. Bransby, A velocity field for some passive earth pressure problems, *Géotechnique*, 21 (1) (1971) 61-83.
- [32] J. Janbu, Soil compressibility as determined by oedometer and triaxial tests, *Proc. ECSMFE, Mexico City, Mexico, Vol. 1 (1963) 191-196.*
- [33] FHWA, *Large Scale Load Tests and Data Base of Five Spread Footings on Sand*, Federal Highway Administration, FHWA, Publication No. FHWA-RD-97-068 Nov. (1997).
- [34] J.-L. Briaud, and R.M. Gibbens, Behavior of five large spread footings in sand, *Journal of Geotechnical and Geoenvironmental Engineering*, ASCE, Vol. 125, 9 (1999) 787-796.
- [35] J.-L. Briaud, Spread footings in sand: load settlement curve approach, *Journal of Geotechnical and Geoenvironmental Engineering*, ASCE Vol. 133, 8 (2007) 905-920.
- [36] M. Veiskarami, Stress level based prediction of load-displacement behavior and bearing capacity of foundations by ZEL Method, *Ph.D. Dissertation*, Submitted to the Department of Civil and Environmental Engineering, Shiraz University, 2010.
- [37] J.-L. Briaud and P. Jeanjean, Load settlement curve method for spread footings on sand, *Geotechnical Special Publication No. 40*, Ed. A. T. Yeung and G. Y. Felio, American Society of Civil Engineers, Reston, Virginia, USA (1994) 1774-1804.



### Appendix-A: Finite difference forms of the equations

Regarding the ZEL equations, there are four equations and four unknowns at each point, e.g., point *C*. A triple point strategy is used to solve the ZEL equations by which, the required data at the third point, i.e., *C* are computed by given data at previous two points, namely *A* and *B*. For terms without a subscript index, the averaged values between two successive points were used. For example, angle  $\psi$  is initially set equal to  $\psi_A$  and after the first round of iteration, it sets equal to averaged value of  $\psi_A$  and  $\psi_C$  along the positive direction.

$$\left\{ \begin{array}{l} \text{For +tive ZEL: } \frac{(z_C - z_A)}{(r_C - x_A)} = \tan(\psi + \xi) \\ \text{For -tive ZEL: } \frac{(z_C - z_B)}{(r_C - x_B)} = \tan(\psi - \xi) \end{array} \right. \quad (A1)$$

Jahanandish (2003) Equations:

$$\left\{ \begin{array}{l} \text{Along the plus (+) ZEL:} \\ (S_C - S_A) + \frac{(T_C - T_B)}{\Delta_{BC}} \Delta_{AC} + \frac{2T}{\cos \nu} ((\psi_C - \psi_A) - \sin \nu \frac{(\psi_C - \psi_B)}{\Delta_{BC}} \Delta_{AC}) = [f_r \cos(\psi + \xi) + f_z \sin(\psi + \xi)] \Delta_{AC} \\ \text{Along the minus (-) ZEL:} \\ (S_C - S_B) + \frac{(T_C - T_A)}{\Delta_{AC}} \Delta_{BC} - \frac{2T}{\cos \nu} ((\psi_C - \psi_B) - \sin \nu \frac{(\psi_C - \psi_A)}{\Delta_{AC}} \Delta_{BC}) = [f_r \cos(\psi - \xi) + f_z \sin(\psi - \xi)] \Delta_{BC} \end{array} \right. \quad (A2)$$

$$\left\{ \begin{array}{l} \Delta_{AC} = \sqrt{(r_A - r_C)^2 + (z_A - z_C)^2} = d\varepsilon^+ \\ \Delta_{BC} = \sqrt{(r_B - r_C)^2 + (z_B - z_C)^2} = d\varepsilon^- \end{array} \right. \quad (A3)$$

Displacement equations:

$$\begin{aligned} dudr + dvdz &= 0 \\ \Rightarrow \left\{ \begin{array}{l} (u_C - u_A)(r_C - r_A) + (v_C - v_A)(z_C - z_A) = 0 \\ (u_C - u_B)(r_C - r_B) + (v_C - v_B)(z_C - z_B) = 0 \end{array} \right. \end{aligned} \quad (A4)$$

Shear strain computation can be done by the following equation [30]:

$$\gamma_{rz} = \frac{\left( \cos(\psi + \xi) \frac{\partial u}{\partial \varepsilon^-} - \cos(\psi - \xi) \frac{\partial u}{\partial \varepsilon^+} - \sin(\psi + \xi) \frac{\partial v}{\partial \varepsilon^-} + \sin(\psi - \xi) \frac{\partial v}{\partial \varepsilon^+} \right)}{\cos \nu} \quad (A5)$$

Therefore, the finite difference form of this equation will be as follow:

$$\gamma_{rz} = \frac{\left( \cos(\psi + \xi) \frac{u_C - u_B}{\Delta_{BC}} - \cos(\psi - \xi) \frac{u_C - u_A}{\Delta_{AC}} - \sin(\psi + \xi) \frac{v_C - v_B}{\Delta_{BC}} + \sin(\psi - \xi) \frac{v_C - v_A}{\Delta_{AC}} \right)}{\cos \nu} \quad (A6)$$

Finite difference forms of the ZEL equations are programmed as supplementary functions in the developed computer code. The following supplementary functions have been coded:

- Function ZELCALC: In this function, the ZEL directions are first computed from equation. A1 and then, the stresses are computed from equation A2 and equation A3. An iterative procedure is carried out for convergence since the values of  $\psi$  are stress dependent and therefore, coordinates of the third point, *C*, depend on the computed stresses.

- Function DISCALC: In this function, the displacement field is computed. When the displacement boundary is known, a similar triple point strategy is performed to solve two unknown displacement components of point  $C$ , namely,  $u_c$  and  $v_c$  by equation A4. In the same function, maximum shear strains at each point are also computed by using equation A6.
- Function PHIFUN: In this function, a soil model can be inserted to compute the appropriate values of soil mobilized friction angle as a function of both stress level and maximum shear strain.

A general iterative procedure is also carried out over the entire loop (at each displacement step) until no significant change is observed in the values of stresses and other unknowns. The flowchart of the calculation procedure is outlined below:

